Afropolitan Journals

ISSN: 3027-2882 www.afropolitanjournals.com

Reactive Power Compensation Using STATCOM and Instantaneous Reactive Power Theory

Abdulrahman Mohammed Galadima

Department of Electrical and Electronics Engineering Technology, Federal Polytechnic Mubi, Nigeria.

Corresponding author: amgaladima@gmail.com

DOI: *https://doi.org/10.62154/ajastr.2025.018.010672*

Abstract

Reactive power can have a range of negative impacts on energy generation and consumption in a power system network. These include creating unnecessary increases in generation, leading to the overall decline in grid efficiency and significant resource inefficiencies. Reactive power compensation is, therefore, critical for improved system performance and elevated productivity. This research aims to design and simulate a 3-phase reactive power compensation model using a Static Synchronous Compensator (STATCOM) to improve the system's power factor and effectively suppress the system harmonics. This is implemented using MATLAB/Simulink software in which the STATCOM is connected to a 3-phase load system fed from a 500 kVA, 11kV/400V source. Based on an instantaneous reactive power (IRPT) theory, the load reactive power is harnessed to generate an inverted signal that will drive the gates of the semiconductor devices of the STATCOM inverter to cancel out the reactive current consumed by the load. Initially, a purely resistive load is connected to the system, where the model response is observed through the Simulink display blocks. Subsequently, an incremental amount of reactive load is added in three steps: 4126 Var, 8576 Var and 13470 Var, respectively. In each case, the model's response is observed and analyzed. The results show that the model can instantly generate and compensate for the equivalent load reactive power, improving the power factor from 0.87, 0.84 and 0.81, respectively, to 1.0. Using a Fast Fourier Transform (FFT) signal analyzer, the system's total harmonic distortion (THD) is improved from 14.22% to 0.22%. This conforms to the IEEE 519 standard limit of 5.0%.

Keywords: Reactive Power, STATCOM, Power Factor, Harmonic Distortions, MATLAB, Instantaneous Reactive Power Theory (IRPT).

tetfund TERTIARY EDUCATION TRUST FUND

Introduction

In recent years, energy demand has grown exponentially while supply has struggled to keep pace due to various challenges, particularly in low and emerging economies (Ali & Ali, 2022; Galadima et al., 2023; Zican Tao, 2024). This can be observed in the power sector, where

system networks repeatedly lose stability due to energy imbalance caused by reactive power issues. Reactive power is essential for the stable operation of AC power systems, as it supports voltage regulation and enables the proper functioning of electrical equipment like motors and transformers. Unlike real power, which performs useful work, reactive power does not directly contribute to energy consumption but is necessary for maintaining voltage levels and system stability. This power component is generated by inductive and capacitive components and must be carefully managed to ensure system efficiency and prevent voltage instability (Herrera-perez et al., 2023; Hosseinzadeh et al., 2021).

The power triangle, shown in Figure 1, visualizes the relationship between real power (P), reactive power (Q), and apparent power (S) in AC circuits (Adepu et al., 2019).

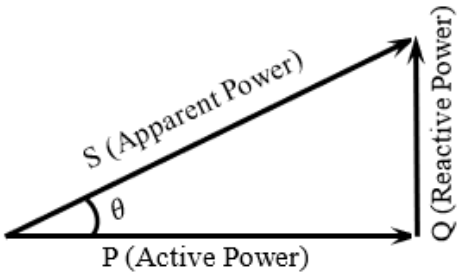

Figure 1: Power triangle showing the vectorial relationship between *P*, *Q* and *S*

Mathematically, these components follow the Pythagorean theorem, expressed as:

$$S^2 = P^2 + Q^2 \qquad (1)$$

From this expression, the apparent power (*S*) consists of real power (*P*), which performs valuable work, and reactive power (*Q*), which oscillates between the source and the load without contributing to actual work. The power factor is given by:

$$Power\ factor\ (PF) = cos\theta = \frac{P}{S} \qquad (2)$$

This equation indicates that a high reactive power (*Q*) reduces the power factor, increasing the total apparent power (*S*) required for the same real power (*P*). This inefficiency leads to increased line losses due to higher current flow, reduced power network voltage stability, and higher capacity requirements for network components.

To improve efficiency, reactive power compensation is implemented to reduce *Q*, thereby improving the power factor ($cos\theta$). This can be illustrated mathematically:

If compensation reduces Q, the new apparent power (S′) becomes:

$$S' = \sqrt{P^2 + (Q - Q_C)^2} \qquad (3)$$

Where Q_C is the compensated reactive power. Since S' is now smaller, the power factor improves:

$$cos\theta' = \frac{P}{S'} \qquad (4)$$

In more detail, Figure 2 illustrates two sets of a simple power system where an induction motor is fed from a utility to demonstrate the benefit of reactive power compensation. In

Figure 2 (a), the reactive power requirement of the load is taken directly from the utility, which forces it to deliver the undesired 100% or more of its rated capacity. In Figure 2 (b), on the other hand, the utility is relieved of the stress of generating the reactive power requirement of the load by connecting a compensator near the load center.

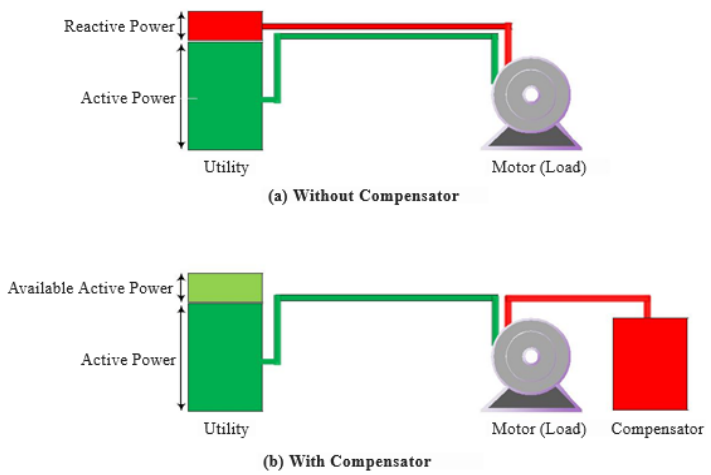

Figure 2: The benefit of reactive power compensation in a power system network

Reactive power is, indeed, taking a new incremental dimension in recent years as a result of two factors: an increased penetration of variable renewable energy sources such as solar/wind and an expanding demand for power electronics due to technological advancements (Alex, 2021; Tang et al., 2022). In 2023, for example, over 40% of the world's electricity was generated from zero-carbon sources. Renewable energy, including wind and solar, contributed 17% to the total electricity generation, while hydroelectric and nuclear power added another 24%. As shown in figure 3, solar and wind accounted for more than 90% of global energy capacity additions during that year (Brown, 2024).

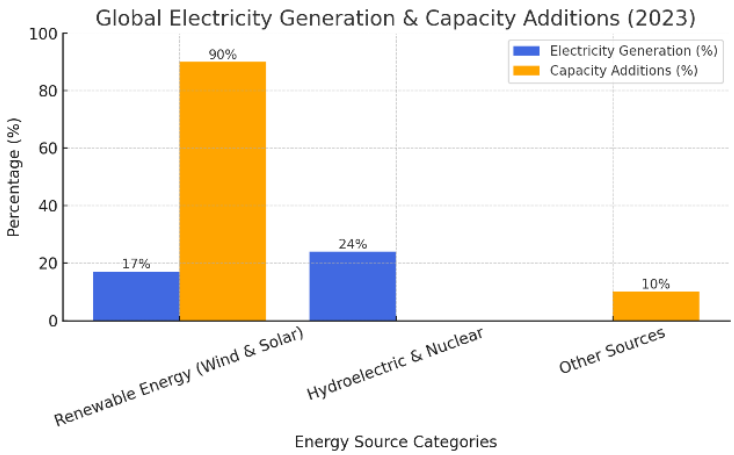

Figure 3: Global Electricity Generation & Capacity Additions (2023)

Note. Adapted from *Global Energy Transformation: A Roadmap to 2050* (p. 25), by International Renewable Energy Agency, 2024, retrieved from https://www.irena.org/publications/2024/Mar/Global-Energy-Transformation-A-Roadmap-to-2050. Copyright 2024 by IRENA.

The global power electronics market was valued at approximately USD 52.70 billion in 2022. It is projected to grow to USD 153.30 billion by 2030, registering a compound annual growth rate (CAGR) of 13.8% during the forecast period from 2023 to 2030(GLOBE NEWSWIRE, 2023). Another analysis forecasts the market to expand from USD 46.2 billion in 2023 to USD 61.0 billion by 2028, with a CAGR of 5.7% (MarketsandMarkets, 2023).

Statement of the Problem

The increasing demand for reactive power in modern electrical grids has led to significant transmission losses and reduced power efficiency. Traditional compensation techniques, such as fixed capacitor banks and SVCs (Static VAR Compensators), have limitations in dynamic response and adaptability to rapidly changing load conditions.

STATCOM has emerged as an effective solution for dynamic reactive power compensation due to its fast response, high controllability, and ability to improve power factor and voltage regulation. However, efficient control of STATCOM for real-time compensation requires an advanced control strategy. The Instantaneous Reactive Power Theory (IRPT), also known as the p-q theory, provides a robust mathematical framework for real-time analyzing and controlling reactive power in 3-phase power systems.

Despite its potential, integrating IRPT with STATCOM for optimal reactive power compensation remains an area that requires further research. To fully leverage this approach's benefits, challenges such as accurate real-time computation, noise sensitivity, and implementation complexities must be addressed.

This study aims to develop an enhanced reactive power compensation strategy by integrating STATCOM with Instantaneous Reactive Power Theory, analyzing its performance under various load conditions, and demonstrating its effectiveness in improving voltage stability, power quality, and overall system efficiency.

Objectives of the Study

1. To design and simulate a STATCOM capable of generating and injecting the reactive power required by a 3-phase load, thereby improving the load power factor to unity.
2. To design and simulate a STATCOM to reduce harmonic distortions in the system to below 1%, in compliance with IEEE 519 standards, ensuring improved power quality and stability.

Literature Review

Various approaches to compensating system reactive power have been presented in different literature. The most common and popular methods include synchronous generators and passive devices such as capacitor banks and shunt reactors. When capacitors are used for compensation, several units are combined to form a bank connected in a delta or star arrangement. The resulting unit is protected in an enclosure made of non-corrosive metal such as aluminium. The enclosure contains all the necessary auxiliary facilities, such as busbars, insulators, etc. Depending on the size of the bank, this can be placed at the load end or the point of common coupling (Ayalew et al., 2019; Kumar & Buwa, 2020; S Mani Kuchibhatla, 2022). An improved capacitor performance with better compensation efficiency can be achieved through various techniques, such as those presented in (Bayat & Bagheri, 2019). In a similar study, (Al-Jubori & Hussain, 2020) established an enhanced method called the Dolphin Optimization Algorithm (DOA), which involves appropriately selecting the sizes and locations of capacitor banks. Using two case studies—the IEEE 16-bus and the 33-bus—they assessed various load models and obtained the best reactive power compensation. (Medina-Gaitán et al., 2023) have also conducted similar research to optimize reactive power compensation with fixed-step capacitor banks using the black hole optimization (BOH) technique. Although capacitor banks have the advantages of cost, installation, and maintenance simplicity, these studies revealed some shortfalls of fixed Compensation, Harmonic Resonance, Voltage Rise Issues, Switching Transients, Limited dynamics, and Aging and degradation.

A new approach to improving the power factor of both leading and lagging loads that employ PIC Microcontroller has been implemented by (Ehsan et al., 2019). A primary requirement in implementing this method is figuring out the zero crossing of voltage and current signals. The capacitive and inductive banks are then used to compensate for the reactive power according to the reactive load type. This approach is also associated with the issue of the accuracy of response to the variations in the system's reactive power. In an attempt to remedy these challenges, (Ali et al., 2021) and (Mane et al., 2020) have developed an automatic power factor correction (APFC) system of capacitor banks that dynamically monitors and establishes a required level of the system's power factor. The APFC uses a microcontroller programmed to track the load power factor at a predetermined level. Integrating capacitor banks with a microcontroller reduces switching transients by optimizing capacitor bank switching sequences but involves a higher initial cost. In some applications, the performance of the reactive capacitors is also facilitated through modern information and communication technology (ICT) gadgets. This accelerates the remote control and reconfigurations of the capacitor banks (Coman et al., 2020). However, electromagnetic interference can easily affect the performance of the ICT gadgets which may lead to poor output of the reactive capacitors.

Synchronous condensers are also popular in reactive power compensation applications. Depending on the excitation of the filed winding, they can be configured to supply or absorb

reactive power. When the field is under-excited, the synchronous Generator absorbs reactive power; when over-excited, it supplies reactive power. The generators have an advantage (over capacitor banks) of providing a relatively more accurate required amount of reactive power with much fewer auxiliary devices. Researches are conducted virtually, and new implementation strategies are being put in different positions in the power system network (Albatran & Al-shorman, 2023; Dai et al., 2020). For instance, in a recent work of (Zican Tao, 2024), synchronous condensers are used to optimize HVDC transmission based on the reactive power conversion factor. The research examines how initial reactive power settings influence dynamic reactive power reserves. Similar studies have also been conducted recently by (Ye, L and Longfu, 2024), (Y. Xu, X. Pan, J. Guo, 2023) and (X. Zhou, K. Wei, 2018) which focus on optimizing the performance characteristics of the synchronous condensers through various control schemes, such as sliding mode control, the Artificial Fish Swarm (AFS) algorithm, and some reliable mathematical models. Due to inertia, the machines are associated with slow response time, high mechanical and electrical losses, poor harmonic handling, and also high implementation costs.

Some academic papers demonstrated the ability to manage reactive power with conventional STATCOMs, utilizing various control strategies. (Srikakolapu et al., 2022) For example, designed and implemented distribution-STATCOM (DSTATCOM) using predictive control, integrated with a multi-criterion decision-making technique. This work, however, is limited to harmonic load-triggered reactive power. A similar study conducted by (Khalaj Monfared et al., 2022) yields results with a similar shortcoming. The concept of a proportional-integral (PI) controller in managing the distributed STATCOM has also been explored in literature, such as in (Igbinovia et al., 2015). This control approach has shown some improvement to the predictive control approach. While widely utilized, proportional-integral (PI) control methods exhibit certain limitations, such as a lack of the derivative component, which is essential for predicting system behaviour and mitigating rapid changes in error. This can lead to poor response times and decreased stability in dynamic conditions. An additional limitation is exhibited in (Eswarana & Kumar, 2017), where the integral term accumulates excessively during sustained errors. This introduces a significant overshoot and prolonged settling times in their result. These constraints suggest that PI control methods may be inadequate for applications requiring swift and precise responses to fluctuating conditions.

This literature review examines and compares Instantaneous Reactive Power Theory (IRPT)-based STATCOM with conventional STATCOM, Static VAR Compensator (SVC), capacitor banks, and synchronous condensers, emphasizing control strategies, response time, harmonic mitigation, and implementation feasibility. Table 1 summarizes the comparative analysis of the various reactive power compensation techniques.

Table 1: Comparative analysis of IRPT-based STATCOM, Conventional STATCOM and other Techniques

FEATURE	IRPT-Based STATCOM	Conventional STATCOM	SVC (Static VAR Compensator)	Capacitor Banks	Synchronous Condenser
CONTROL STRATEGY	Uses IRPT for instantaneous compensation	Uses PI controllers or predictive control	Thyristor-controlled reactor (TCR) and thyristor-switched capacitor (TSC)	Fixed or switched capacitor-based compensation	Rotating synchronous machine providing dynamic reactive power
RESPONSE TIME	Ultra-fast, cycle-by-cycle compensation	Fast, within a few cycles	Moderate, depends on thyristor switching	Slow, step-wise switching	Slow, due to mechanical inertia
HARMONIC FILTERING	Excellent, actively filters harmonics	Moderate, depending on the control method	Poor, may introduce harmonics	May amplify harmonics due to resonance	Good, but may require additional filters
DYNAMIC LOAD HANDLING	Highly adaptive to rapid load changes	Adaptive but slower than IRPT	Moderate, slower response to load variations	Poor, best suited for steady loads	Good, but slower than STATCOM-based solutions
VOLTAGE REGULATION	Superior, ensures effective voltage stability	Good, slightly slower response	Moderate, may introduce voltage fluctuations	Poor, may lead to overvoltage issues at low loads	Excellent, provides inertia support
COMPENSATION ACCURACY	High, utilizes instantaneous reactive power calculations	High, but depends on controller tuning	Moderate, limited by thyristor control	Low, provides only fixed compensation	High, depends on excitation control
SYSTEM LOSSES	Moderate, due to power electronics losses	Moderate, similar to IRPT-based STATCOM	Low, but thyristor switching causes losses	Low, though overcompensation may increase losses	High, due to mechanical and electrical losses
IMPLEMENTATION COST	High, requires DSP/microcontroller-based control	High, due to complex power electronics	Moderate, more affordable than STATCOM but costlier than capacitors	Low, most cost-effective	Very high, due to equipment and maintenance costs
RELIABILITY	High, robust under varying conditions	High, dependent on power electronics durability	Moderate, thyristor failure may affect performance	Very high, though capacitors degrade over time	Very high, but requires frequent maintenance
SPACE REQUIREMENT	Compact, modular design	Compact, similar to IRPT-based STATCOM	Large, requires reactors and capacitors	Very large, especially for high compensation needs	Very large, due to rotating machinery requirements

As noted in the analytical table, other compensation features often have numerous limitations, mainly the inability to integrate reactive power compensation and excellent harmonic filtering. These deficiencies can lead to inadequate voltage regulation and increased system losses, particularly under dynamic load conditions. Addressing these challenges necessitates the development of more adaptive and responsive compensation solutions, such as IRPT-based STATCOM. This choice employs the IRPT-based algorithm to

calculate and compensate reactive power instantaneously, which is responsible for numerous advantages, such as ultra-fast response time, superior harmonic filtering, and high adaptability to dynamic loads.

Methodology

To achieve the listed objectives, the following methodology was adopted: a 3-phase generation rated 11kV/400V, 50Hz feeding a system of inductive loads with a given level of reactive power consumption was modelled using MATLAB/Simulink software. This software was chosen for this study due to its advantages in power electronics circuits and systems in modelling, simulation, analysis, design, optimization, parameter tuning, real-time implementation, hardware testing, etc. Some of these advantages include but are not limited to the following:

- Integrated power electronics and control system design: Unlike PSIM (optimized for power circuits) or PSCAD (better suited for transient analysis), MATLAB/Simulink enables simultaneous modelling of power converters, controllers, and grid interactions using Simscape electrical and control system toolbox.
- Accurate dynamic simulation: MATLAB's variable-step solvers ensure high-fidelity simulation of STATCOM's transient and steady-state solvers, outperforming fixed-step solvers in PSIM and LTspice, which may compromise accuracy.
- Advanced Control and Optimization: The platform supports P, PI, PID and adaptive control schemes, offering superior flexibility compared to PSCAD, which is limited in control design.
- Widely adapted in industry and Academia: MATLAB/Simulink is widely used in electrical and electronic engineering research and industry, ensuring better documentation, support, and collaboration opportunities for the study.

Using the software, the STATCOM, which is connected across the supply-load line at the point of common coupling (PCC), was modelled. The complete schematic diagram is illustrated in Figure 4.

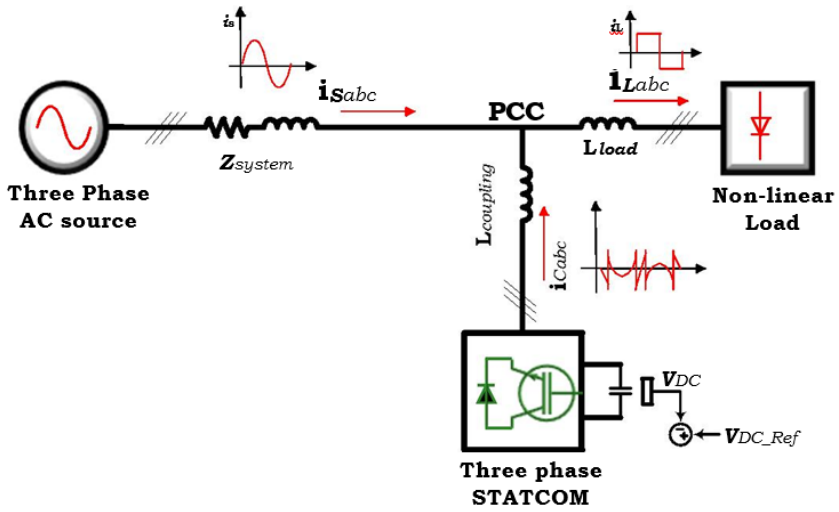

Figure 4: Schematic diagram of a 3-phase STATCOM connected at PCC

The figure shows that the STATCOM is set in a closed-loop control to dynamically regulate the system's power factor by injecting or absorbing reactive power for a maintained, balanced supply-load relationship. This is based on an IRPT, which allows for calculating both active (p) and reactive power (q) at any given time. The block diagram in Figure 5 illustrates the sequence involved in this operation.

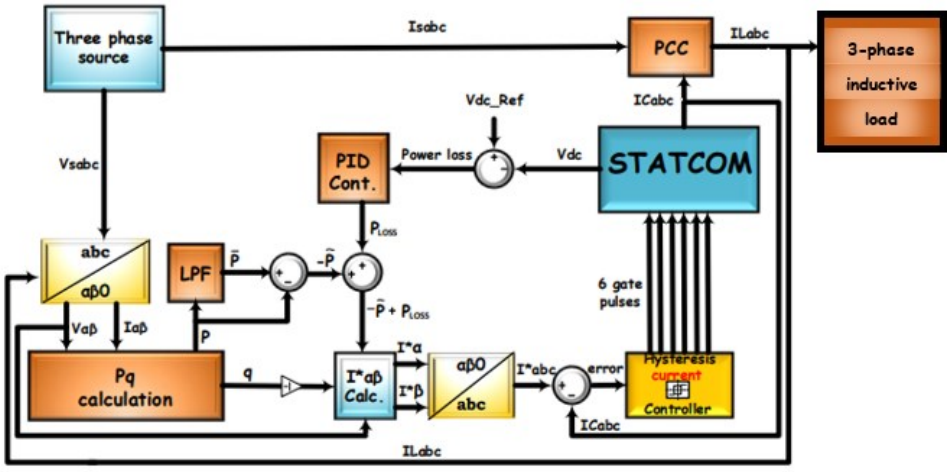

Figure 5: Block diagram of the STATCOM illustrating the interrelation of the system components and the flow of operational sequence

The first step in the operational phases of the diagram is the conversion of the 3-phase inductive load currents $\boldsymbol{I}_{\mathbf{Labc}}$ and the source voltage $\boldsymbol{V}_{\mathbf{Sabc}}$ to a 2-phase orthogonal ($\alpha\beta 0$) fixed reference frame. This simplifies mathematical calculations and facilitates the control of the STATCOM inverter. This is shown in the abc-to- $\alpha\beta 0$ block. The 2-phase frame is used to extract the system's instantaneous active and reactive power (pq) used for generating

the reference currents (I_α^* and I_β^*) after passing through a low passive filter (LPF). This 2-phase frame reference current is then passed through a conversion block to restore the original 3-phase quantities, $\boldsymbol{I}_{abc}^*$. This is called inverse Clark's transformation or $\alpha\beta 0$ -to-*abc.* This reference current is controlled using the hysteresis loop pulse width modulation (PWM) control technique. The current is used to fire the gates of the STATCOM inverter switches to compensate for the system's reactive currents. The main blocks involved in the STATCOM control operation are explained in some detail as follows:

abc-to- $\boldsymbol{\alpha\beta 0}$ block: Clark's Transformation:

The orthogonal components of the system in a stationary reference frame are obtained using the following transformation matrices:

$$\begin{bmatrix} V_o \\ V_\alpha \\ V_\beta \end{bmatrix} = \sqrt{\frac{2}{3}} \begin{bmatrix} \frac{1}{\sqrt{2}} & \frac{1}{\sqrt{2}} & \frac{1}{\sqrt{2}} \\ 1 & -\frac{1}{\sqrt{2}} & -\frac{1}{\sqrt{2}} \\ 0 & \frac{\sqrt{3}}{2} & -\frac{\sqrt{3}}{2} \end{bmatrix} \begin{bmatrix} V_a \\ V_b \\ V_c \end{bmatrix} \quad (5)$$

$$\begin{bmatrix} I_o \\ I_\alpha \\ I_\beta \end{bmatrix} = \sqrt{\frac{2}{3}} \begin{bmatrix} \frac{1}{\sqrt{2}} & \frac{1}{\sqrt{2}} & \frac{1}{\sqrt{2}} \\ 1 & -\frac{1}{\sqrt{2}} & -\frac{1}{\sqrt{2}} \\ 0 & \frac{\sqrt{3}}{2} & -\frac{\sqrt{3}}{2} \end{bmatrix} \begin{bmatrix} V_a \\ V_b \\ V_c \end{bmatrix} \quad (6)$$

Where a, b & c represent the 3-phase input signals and the α & β represent the two orthogonal components; $\sqrt{\frac{2}{3}}$ is a transformation coefficient.

pq block: determination of active (p) and reactive power (q).

In a balanced 3-phase system, the zero sequence components, V_o and I_o become zero. Therefore, the instantaneous p and q are given by:

$$\begin{aligned} p &= V_\alpha I_\alpha + V_\beta I_\beta \\ q &= V_\beta I_\alpha + V_\alpha I_\beta \end{aligned} \quad (7)$$

This can be represented in matrix form as:

$$\begin{bmatrix} p \\ q \end{bmatrix} = \begin{bmatrix} V_\alpha & V_\beta \\ -V_\beta & V_\alpha \end{bmatrix} \begin{bmatrix} I_\alpha \\ I_\beta \end{bmatrix} \quad (8)$$

Now for the fact that the α and β components of current are non-sinusoidal due to inductive load, both active and reactive power will also oscillate, resulting in both linear and sinusoidal components of p and q as shown in equation 9.

$$\begin{aligned} p &= \tilde{P}_{ac} + \bar{p}_{dc} \\ q &= \tilde{q}_{ac} + \bar{q}_{dc} \end{aligned} \quad (9)$$

The subscript *ac* and *dc* denote oscillating and linear or dc components of both p and q, respectively.

To optimise the power factor, the negative components of $\tilde{P}_{ac}$ and q (i.e., $-\tilde{P}_{ac}$ and $-q$) have to be fed into the system. The value of $\tilde{P}_{ac}$ is obtained through a low pass filter (LPF), while the inversion of q gives the required magnitude of $-q$ as shown in the block diagram. Hence, equation 9 is modified to,

$$\begin{aligned} p &= -\tilde{P}_{ac} \\ q &= -q \end{aligned} \qquad (10)$$

From equation 8, we have:

$$\begin{bmatrix} I_\alpha \\ I_\beta \end{bmatrix} = \begin{bmatrix} V_\alpha & V_\beta \\ -V_\beta & V_\alpha \end{bmatrix}^{-1} \begin{bmatrix} p \\ q \end{bmatrix} \qquad (11)$$

Therefore, the orthogonal components (α and β) of the reference currents required for controlling the STATCOM inverter switches is:

$$\begin{bmatrix} I_\alpha^* \\ I_\beta^* \end{bmatrix} = \frac{1}{V_\alpha^2 + V_\beta^2} \begin{bmatrix} V_\alpha & -V_\beta \\ V_\beta & V_\alpha \end{bmatrix}^{-1} \begin{bmatrix} p \\ q \end{bmatrix} \qquad (12)$$

Substituting the magnitude of p and q in equation 10, we have:

$$\begin{bmatrix} I_\alpha^* \\ I_\beta^* \end{bmatrix} = \frac{1}{V_\alpha^2 + V_\beta^2} \begin{bmatrix} V_\alpha & -V_\beta \\ V_\beta & V_\alpha \end{bmatrix}^{-1} \begin{bmatrix} -\tilde{P}_{ac} + p_{loss} \\ -q \end{bmatrix} \qquad (13)$$

p_{loss} is the average power loss due to the switching operation of STATCOM's semiconductor devices? This will ensure a regulated DC bus voltage, as the diagram shows. The established reference currents in equation 13 are converted to their corresponding 3-phase signals, I_{abc}^* yielding equation 14. The diagram illustrates this step as the inverse of Clark's transformation block.

$$\begin{bmatrix} I_a^* \\ I_b^* \\ I_c^* \end{bmatrix} = \sqrt{\frac{2}{3}} \begin{bmatrix} 1 & 0 \\ -\frac{1}{2} & \frac{\sqrt{3}}{2} \\ -\frac{1}{2} & \frac{\sqrt{3}}{2} \end{bmatrix} \begin{bmatrix} I_\alpha^* \\ I_\beta^* \end{bmatrix} \qquad (14)$$

These are the required currents for driving the STATCOM inverter switches (IGBTs).

Control of the switching currents (I_{abc}^*) using the hystereses technique

For steady operation of the inverter switches, ripple-free firing signals are necessary. This work selects a reliable and easier control technique known as Hysteresis PWM control, shown in Figure 6.

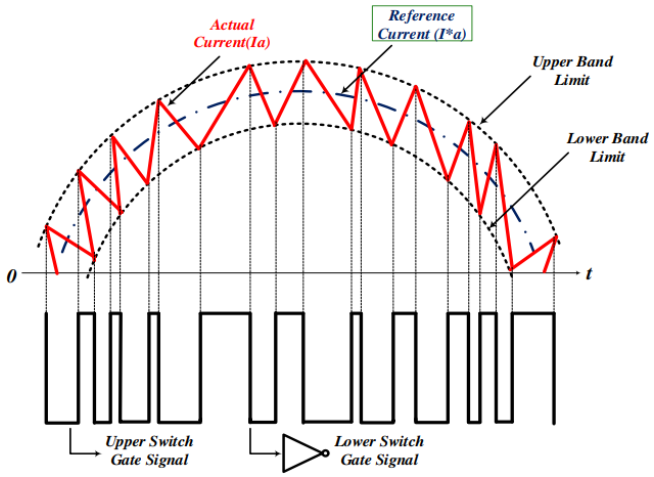

Figure 6: Semi-sinusoid illustration of Hysteresis PWM current control

Note. Adapted from Journal of Applied Materials and Technology by Kabir, I., Jibril, Y., Abubakar, A. S., & Olarinoye, G. A. (2024). Exploring the Potentials and Drawbacks of Hysteresis Current Controller for SRM: A Case Study of Wind Energy Conversion System. *Journal of Applied Materials and Technology*, 5(2), 41–48.

The figure elaborates a half-cycle sinusoidal signal of one of the phases with a pulse-width modulated signal, switching ON and OFF in a complementary fashion with a bandwidth determined by the hysteresis lower and upper limits, as shown *(Kabir et al., 2024)*. I_a is the actual inverter switching current and I_a^* is the set (reference) current. For example, when I_a reaches the upper limit, the upper switch opens, and the lower switch will instantly close. The reverse is the case when the I_a reaches the lower limit. This process continues to ensure the switching is maintained at the reference current.

Determination of STATCOM System Design Parameters

The following are the initial values typically assumed or obtained based on the system requirements:

i. V_s, the line-to-line voltage of the power system where the STATCOM is connected $= 400\ V$.
ii. Reactive power compensation capacity (Q) $= 200\ kVar$.
iii. Modulation Index (m).
iv. Switching Frequency (f_s) Chosen based on power electronic switching devices (IGBT in this case).
v. $V_{STATCOM}$, typically higher than V_s for effective reactive power compensation.

The following are derived/calculated parameters based on the set parameters:

- **Inverter DC bus voltage**

For a 3-phase line voltage, equation 15 relates the DC bus voltage, RMS line voltage and the modulation index (m).

$$V_{DC} \geq \frac{2\sqrt{2}V_{LL}}{\sqrt{3} \cdot m} \qquad (15)$$

$$\therefore \quad V_{DC} \geq \frac{2 \times \sqrt{2} \times 400}{\sqrt{3} \times 1} \approx \mathbf{650\ V} \qquad \text{(For a modulation index of 1)}$$

- **Inverter DC link capacitor**

Using the ripple voltage method, the STATCOM inverter's DC link capacitor is given by equation 16.

$$C_{DC} = \frac{I_{DC}}{2f_{sw}\Delta V_{DC}} \qquad (16)$$

Where:

I_{DC} = DC bus current in Amps $= \frac{reactive\ power\ rating\ of\ the\ STATCOM}{V_{DC}} = \frac{200kVar}{650V} = 307.69A$.

f_{sw} = Switching frequency in Hz (1.6 kHz is selected for an insulated gate bipolar transistor (IGBT) switch used in the simulation)

ΔV_{DC} = Allowable DC voltage ripple in Volts (2.5% of 650V = 16.25 V).

$$\therefore \quad C_{DC} = \frac{307.69\ A}{2 \times 1.6\ kHz \times 16.25\ V} = 5{,}916.7\ \mu F \approx \mathbf{6{,}000\ \mu F}$$

- **Coupling Reactance**

The required coupling inductance (X_L) was determined from the reactive power exchange formula:

$$Q = \frac{V_{system} \times (V_{STATCOM} - V_{system})}{X_L} \qquad (17)$$

Where:

Q is the reactive power rating of the inverter = 200 kVar.

V_{system} is the system's line voltage = 400 V.

$V_{STATCOM}$ is the STATCOM's output voltage, assumed 600 V.

X_L is the inductive reactance of the coupling inductor, hence:

$$X_L = \frac{V_{system} \times (V_{STATCOM} - V_{system})}{Q} = \frac{400\ V \times (600 - 400)\ V}{200 \times 10^3\ VAar} = 0.4\Omega$$

$$\therefore \quad L = \frac{X_L}{2\pi f} = \frac{0.4}{2 \times \pi \times 50} = 1.27 \times 10^{-3} H\ or\ 1.27\ mH$$

- **Selection of K_p and Integral K_i for the PID controller**

An empirical tuning approach was used to determine the proportional (K_p) and integral (K_i) gains of the controller. The K_p value was initially set at 0.1 and incremented in steps of 0.1

to achieve a fast response with minimal oscillations. At $K_p = 1$, K_i was gradually increased until $K_i = 25$, effectively eliminating steady-state error while avoiding excessive overshoot.

Based on these and other design parameters, the system was implemented using MATLAB/Simulink software.

Results and Discussion

Simulation Results

Figure 7 shows the Simulink model illustrating four (4) significant blocks, such as the STATCOM, supply, load, and control systems. The PCC is the point at which the STATCOM injects the compensating currents for instantaneous reactive power adjustment. Figures 8 through 11 illustrate the Simulink display of the STATCOM's dynamic response under varying load conditions.

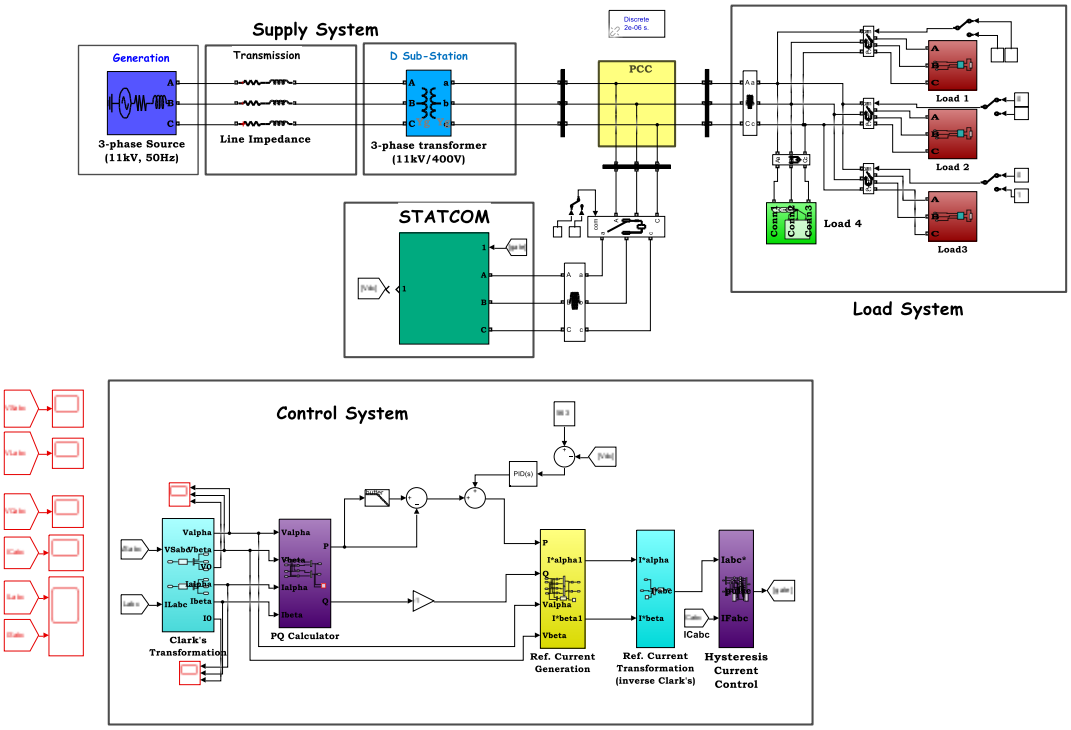

Figure 7: Simulink model of the complete system illustrating the major sub-systems

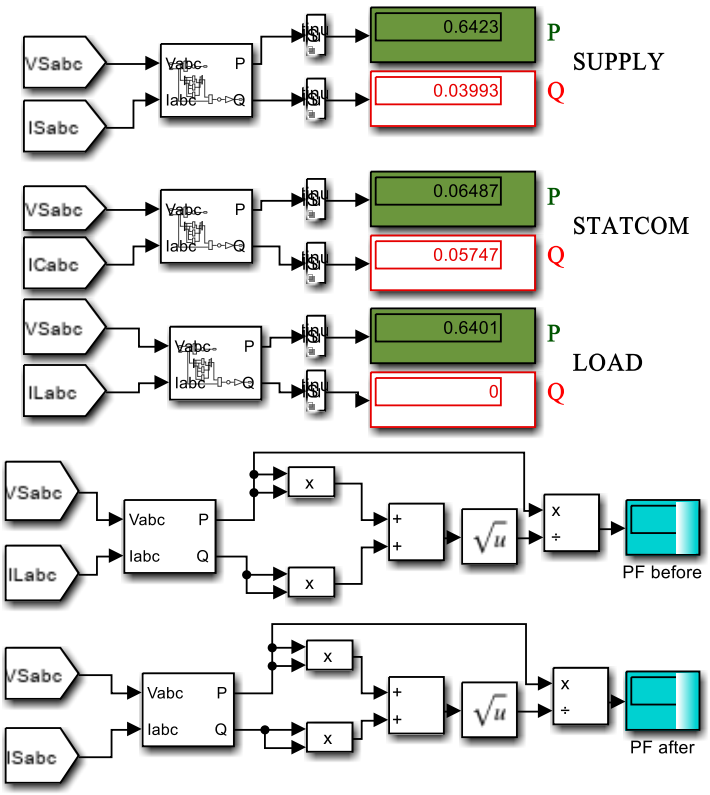

Figure 8: Simulink output for a purely resistive load (**load 4**)

(a) Without STATCOM

(b) with STATCOM

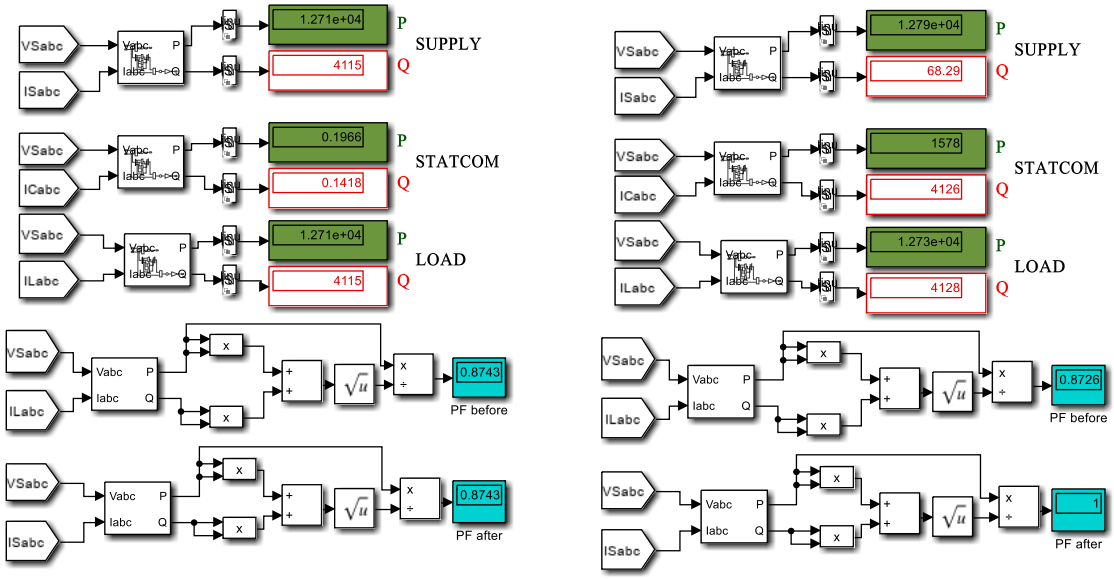

Figure 9: Simulink output when **load 1** (inductive) is added to the system

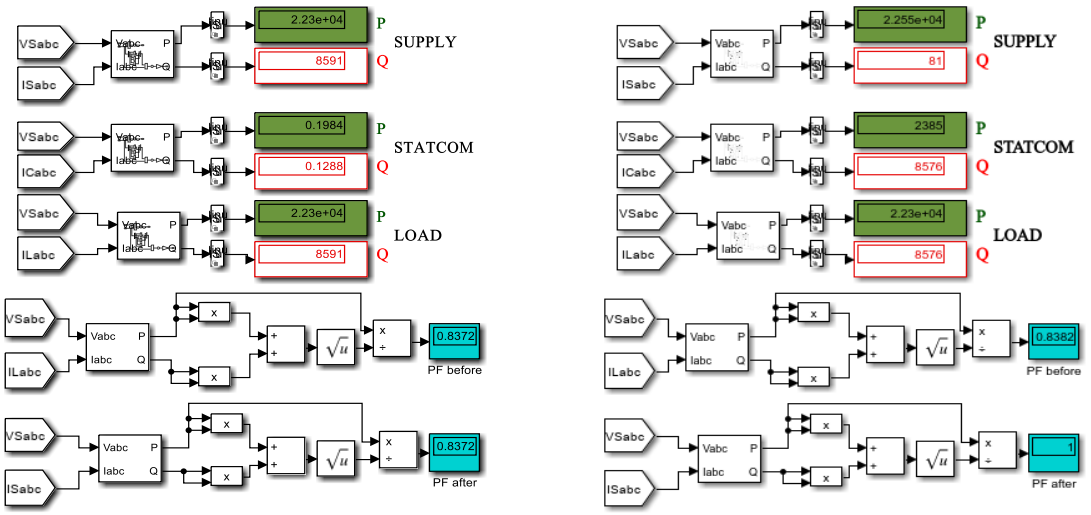

(a) Without STATCOM (b) with STATCOM

Figure 10: Simulink output when **load 2** (inductive) is added to the system

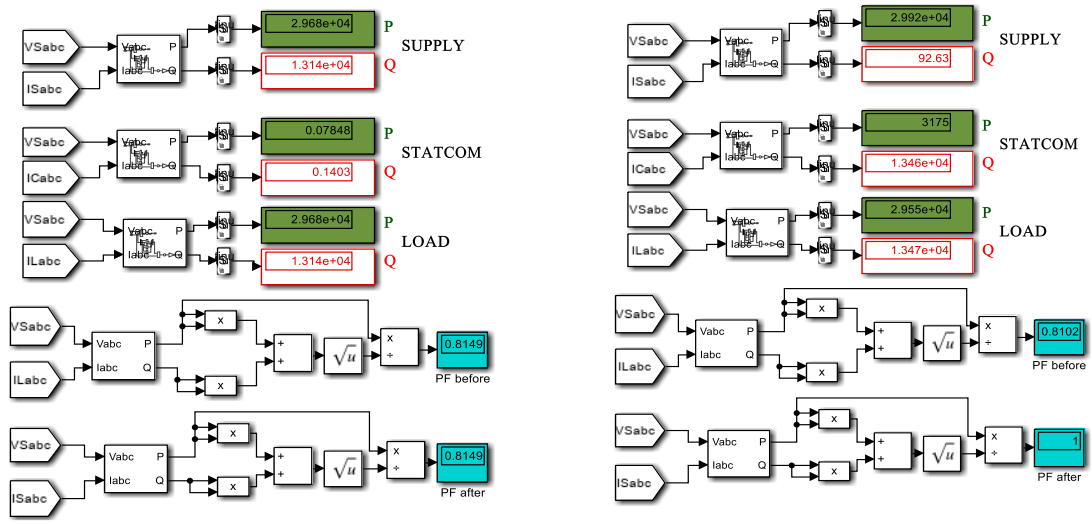

(a) Without STATCOM (b) with STATCOM

Figure 11: Simulink output when **load 3** (inductive) is added to the system

Figures 12 and 15 are the simulation results for the system's performance on harmonic distortion under the full load condition. Figure 12 (a) and (b) are, respectively, the load signal waveforms and the FFT analysis before connecting the STATCOM. Figure 13 (a) and (b) illustrate the corresponding signals and analysis after connecting the STATCOM.

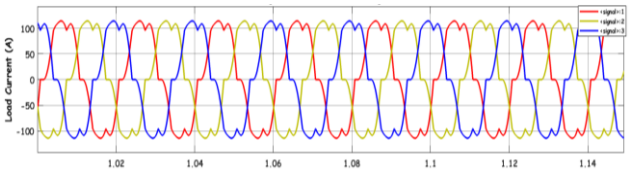

(a) Distorted signal due to harmonic load, which would have replicated on the source current

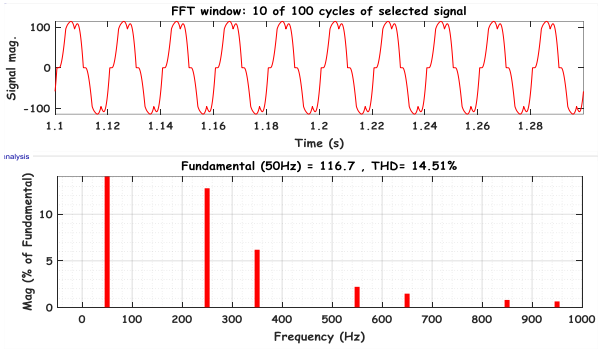

(b) FFT analysis of the harmonic load current signals

Figure 12: Signal waveforms and FFT analysis before compensation

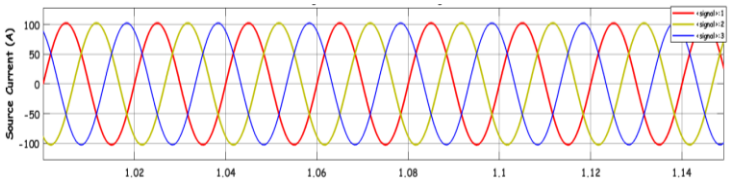

(a) Compensated signal indicated by pure sinusoids

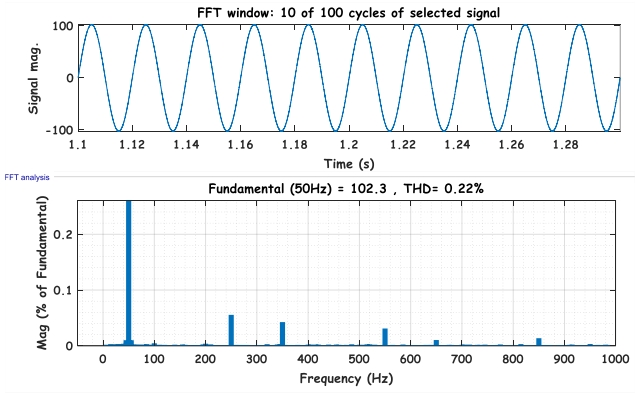

(b) FFT analysis of the signal after compensation

Figure 13: Signal waveforms and FFT analysis after compensation

The Comprehensive Summary of the Results

Table 3 compiles the key performance metrics derived from these simulations under the four load conditions. Similarly, Table 4 compiles the system's performance on harmonic distortion analyses in Figures 12 and 13.

Table 3: The comprehensive summary of the simulink display of Figures 8 through 11

Connected Load	STATCOM Connection	Power Requirement of the load		Power supply by the source		STATCOM Compensation		System Power Factor (PF)	
		(W)	(Var)	(W)	(Var)	(W)	(Var)	Before	After
4 (Purely resistive)	No	0.6401	**0**	0.6423	0.03993	0.06487	0.05747	**1.0**	**1.0**
4+1 (Inductive)*	**No**	12710	**4115**	12710	**4115**	0.1966	0.1418	**0.87**	**0.87**
	Yes	12730	**4126**	12790	68.29	1576	**4126**	**0.87**	**1.0**
4+1+2 (Inductive)*	**No**	22300	**8591**	22300	**8591**	0.1984	0.1288	**0.84**	**0.84**
	Yes	22300	**8576**	22550	81	2385	**8576**	**0.84**	**1.0**
4+1+2+3 (Inductive)*	**No**	29680	**13240**	29680	**13140**	0.07848	0.1403	**0.81**	**0.81**
	Yes	29550	**13470**	29920	92.63	3175	**13460**	**0.81**	**1.0**

Table 4: The STATCOM performance on the system harmonics based on IEEE519 Standard(Galadima et al., 2023)

Harmonic Series	Distortions on the supply side	Distortions on the load side	IEEE 519 Standards (%)
THD	14.5	0.22	5.0
5^{th}	12.8	0.55	4.0
7^{th}	6.18	0.04	4.0
11^{th}	2.22	0.03	2.5
13^{th}	1.48	0.01	2.5
17^{th}	0.81	0.01	1.5
19^{th}	0.65	0.00	1.5

Discussion

Reactive Power Compensation

The performance of the STATCOM on the load reactive power was evaluated using four distinct load configurations: Load 1, Load 2, Load 3, and Load 4. Notably, Load 4 is purely resistive, whereas Loads 1, 2, and 3 are inductive. These inductive loads were incrementally introduced in series to assess varying levels of reactive power consumption, as detailed below:

I. For **Load 4,** characterized as purely resistive, Figure 8 illustrates the corresponding output. In this scenario, the reactive power measures 0 var, aligning with theoretical

expectations. Consequently, the power factor remains at an ideal value of 1.0, both prior to and following STATCOM intervention

II. In the scenario combining **Load 4** (purely resistive) with **Load 1** (inductive), the system's performance was evaluated under two distinct conditions, as depicted in Figures 9(a) and 9(b). Without STATCOM intervention (Figure 9(a)), the source supplied 4,115 var of reactive power, corresponding to a power factor of 0.87, matching the reactive power demand of the load. Upon integrating the STATCOM (Figure 9(b)), it compensated 4,126 var, achieving an ideal power factor of 1.0. These findings are detailed in Row 3 of Table 3.

III. In the scenario combining **Load 4** (purely resistive) with L**oads 1** and **2** (inductive), the system's performance was evaluated under two conditions, as depicted in Figures 10(a) and 10(b). Without STATCOM intervention (Figure 10(a)), the source supplied 8,591 var of reactive power, corresponding to a power factor of 0.84, matching the reactive power demand of the combined loads. Upon integrating the STATCOM (Figure 10(b)), it compensated 8,576 var, achieving an ideal power factor of 1.0.

IV. "Finally, in the scenario combining **Load 4** (purely resistive) with **Loads 1**, **2**, and **3** (inductive), the system's performance was evaluated under two conditions, as depicted in Figures 11(a) and 11(b). Without STATCOM intervention (Figure 11(a)), the source supplied 13,470 var of reactive power, corresponding to the reactive power demand of the combined loads. Upon integrating the STATCOM (Figure 11(b)), it compensated approximately 13,460 var, readjusting the power factor to unity, as summarized in the last row of Table 3."

Slight discrepancies in active and reactive power can be observed in each case of the supply, the load, and or the STATCOM when the load changes. This is usually due to Inherent characteristics of the model components, such as slight inductive elements within the circuits. These inconsistencies are well within the limits of simulation errors.

Harmonic Mitigation

Figure 12(a) depicts the 3-phase load current waveforms under the combined condition of all four loads. These waveforms exhibit significant distortion, indicating the presence of harmonics that can adversely affect power quality. Figure 12(b) presents the FFT analysis of these distorted load currents. The FFT decomposes the time-domain signals into their constituent frequency components, revealing the amplitude of each harmonic present. This analysis is crucial for identifying specific harmonics contributing to the observed distortion. Figure 13(a) illustrates the source current waveforms after the injection of compensating signals at the PCC. Post-compensation, the source currents approximate sinusoidal waveforms, indicating effective mitigation of distortions. Figure 13(b) displays the FFT analysis of the compensated source currents. The significant reduction in harmonic content confirms the efficacy of the compensation strategy in enhancing power quality.

Table 4 summarizes the harmonic analysis results. Column 1 presents the Total Harmonic Distortion (THD) and individual harmonic components from the 5^{th} to the 19^{th} order, excluding zero-sequence harmonics such as the 3^{rd}, 9^{th}, and 15^{th}, typically occurring in a 3-phase, four-wire systems. The analysis indicates that, prior to STATCOM integration, the THD and the 5^{th} and 7^{th} harmonics exceeded the IEEE 519 recommended limits (as detailed in Column 2). However, after connecting the STATCOM, these harmonic levels were significantly reduced, as shown in Column 3.

Choice of Design Parameters

The DC bus voltage V_{DC} being a critical parameter was appropriately selected to achieve the desired reactive power compensation. The value should be sufficient to produce an AC voltage equal to or greater than the peak of the line-to-line RMS voltage $V_{LL(RMS)}$ of the system. Based on the IGBT switch selected for this work, this value is kept constant at 650V. Reactive power control is achieved by adjusting the modulation index (m) (usually between 0.7 and 1) of the PWM, which in turn varies the amplitude of $V_{STATCOM}$ to control the reactive power flow.

IGBT switches are selected over MOSFETs due to their high-power handling capacity (several kW to MW), high voltage and current ratings, and moderate switching frequencies, which make them suitable for use in STATCOMs. Hence, a switching frequency of 1.6 kHz was selected for the 400 kVA STATCOM inverter.

$V_{STATCOM} = 600$ V: Inverter voltage is typically selected, ensuring it is 1.1 to 1.5 higher than V_s for effective reactive power compensation.

Conclusion

Utilizing MATLAB/Simulink software, a STATCOM model based on Instantaneous Reactive Power Theory (IRPT) was developed. The model demonstrated the ability to sense and instantaneously generate the reactive power required by the load, achieving an ideal 1.0 power factor across various reactive power levels. Additionally, under heavy reactive load conditions, the system maintained a sinusoidal signal with a Total Harmonic Distortion (THD) of less than 1%, aligning with IEEE 519 standards and indicating enhanced power quality and system stability.

This real-time compensation approach enhances power system efficiency and grid stability, making it a valuable solution for modern power networks. The study explicitly highlights STATCOM's practical effectiveness in harmonic mitigation and maintaining sinusoidal waveforms.

This result underscores STATCOM's potential for improving power quality, reducing voltage fluctuations, and enhancing the reliability of industrial and utility-scale power systems.

Recommendations

- Future work should focus on experimental validation of the STATCOM model using hardware implementation or real-time digital simulation to confirm its performance beyond simulations.
- Alternative control strategies like AI-based controllers should be explored and tested for improved response and stability.
- The STATCOM should be integrated with renewable energy sources to assess its effectiveness in mitigating voltage fluctuations and enhancing grid stability.
- Field deployment in an actual power system is recommended to evaluate long-term reliability, grid compliance, and economic feasibility.
- The power supply source cannot instantaneously adjust to load changes, leading to slight model performance errors. Further study may design an additional circuit for improved performance.

References

Adepu, S., Kandasamy, N. K., Zhou, J., & Mathur, A. (2019). *Attacks on Smart Grid : Power Supply Interruption and Malicious Power Attacks on Smart Grid : Power Supply Interruption and Malicious Power Generation*. *June*.

Al-Jubori, W. K. S., & Hussain, A. N. (2020). Optimum reactive power compensation for distribution system using dolphin algorithm considering different load models. *International Journal of Electrical and Computer Engineering*, *10*(5), 5032–5047. https://doi.org/10.11591/IJECE.V10I5.PP5032-5047

Albatran, S., & Al-shorman, H. (2023). Reactive power correction using virtual synchronous generator technique for droop controlled voltage source inverters in islanded microgrid. *Energy Systems*, *14*(2), 391–417. https://doi.org/10.1007/s12667-021-00456-6

Alex, O. (2021). *Revisiting the Economic Growth – Energy Consumption Nexus : Does Globalization Matter ?* https://doi.org/10.1016/j.eneco.2021.105472

Ali, M., & Ali, A. (2022). *Urbanisation and energy consumption in Sub-Saharan Africa*. *October*.

Ali, M., Rashid, F., & Rasheed, S. (2021). Power factor improvement for a three-phase system using reactive power compensation. *Indonesian Journal of Electrical Engineering and Computer Science*, *24*(2), 715–727. https://doi.org/10.11591/ijeecs.v24.i2.pp715-727

Ayalew, F., Hussen, S., & Pasam, G. K. (2019). Reactive Power Compensation: a Review. *International Journal of Engineering Applied Sciences and Technology*, *03*(11), 1–7. https://doi.org/10.33564/ijeast.2019.v03i11.001

Bayat, A., & Bagheri, A. (2019). Optimal active and reactive power allocation in distribution networks using a novel heuristic approach. *Applied Energy*, *233–234*(October 2018), 71–85. https://doi.org/10.1016/j.apenergy.2018.10.030

Brown, H. C. (2024, August 27). More Than 40% of World's Electricity Came From Zero-Carbon Sources in 2023. *THE WALL STREET JOURNAL*. https://www.wsj.com/articles/more-than-40-of-worlds-electricity-came-from-zero-carbon-sources-in-2023-064d434e?utm

Coman, C. M., Florescu, A., & Oancea, C. D. (2020). Improving the efficiency and sustainability of power systems using distributed power factor correction methods. *Sustainability (Switzerland)*, *12*(8), 1–20. https://doi.org/10.3390/SU12083134

Dai, F., Tan, F., Jiang, M., Chen, X., Ma, H., & Chen, M. (2020). Characteristic Analysis and Parameter optimization of Synchronous Condensers. *Asia-Pacific Power and Energy Engineering Conference, APPEEC*, *2020-September*, 3–7. https://doi.org/10.1109/APPEEC48164.2020.9220444

Ehsan, M. T., Anwar, A., Ahsan, F., Ur Rehman, M. A., & Kamran, M. (2019). Pic Microcontroller Based Power Factor Correction for both Leading and Lagging Loads using Compensation Method. *Proceedings of 2019 16th International Bhurban Conference on Applied Sciences and Technology, IBCAST 2019*, 377–383. https://doi.org/10.1109/IBCAST.2019.8667256

Eswarana, T., & Kumar, V. S. (2017). Particle swarm optimization (PSO)-based tuning technique for PI controller for management of a distributed static synchronous compensator (DSTATCOM) for improved dynamic response and power quality. *Journal of Applied Research and Technology*, *15*(2), 70–186. https://doi.org/https://doi.org/10.1016/j.jart.2017.01.011

Galadima, A. R., Binti, R., & Idris, M. (2023). *Comparison of APF and STATCOM for Current Harmonic Mitigation*. *22*(3), 4428.

GLOBE NEWSWIRE. (2023). *Power Electronics Market to Reach USD 153.30 Billion by 2030 | 200 Pages Research Report*. https://www.globenewswire.com/en/news-release/2023/09/18/2744578/0/en/Power-Electronics-Market-to-Reach-USD-153-30-Billion-by-2030-200-Pages-Research-Report.html?utm

Herrera-perez, V., Gavilanes, J., & Hernandez-ambato, J. (2023). *Synchronization and Optimal Operation of a 140 kVA Inverter in On-Grid Mode Using Mamdani Controllers in Cascade Jes us*. *2023*.

Hosseinzadeh, N., Aziz, A., Mahmud, A., & Gargoom, A. (2021). *Voltage Stability of Power Systems with Renewable-Energy Inverter-Based Generators : A Review*.

Igbinovia, F. O., Fandi, G., Švec, J., Müller, Z., & Tlusty, J. (2015). *Comparative Review of Reactive Power Compensation Technologies*. *July*. https://doi.org/10.1109/EPE.2015.7161066

Kabir, I., Jibril, Y., Abubakar, A. S., & Olarinoye, G. A. (2024). *Exploring the Potentials and Drawbacks of Hysteresis Current Controller for SRM : A Case Study of Wind Energy Conversion System*. *5*(2), 41–48.

Khalaj Monfared, K., Neyshabouri, Y., Miremad, A., Ahmadi, S., & Iman-Eini, H. (2022). Optimal Switching-Sequence-Based Model Predictive Control for a Hybrid Multilevel STATCOM. *IEEE Transactions on Industrial Electronics*, *69*(10), 9952–9960. https://doi.org/10.1109/TIE.2022.3146592

Kumar, N., & Buwa, O. (2020). A review on reactive power compensation of distributed energy system. *2020 7th International Conference on Smart Structures and Systems, ICSSS 2020*, 16–21. https://doi.org/10.1109/ICSSS49621.2020.9202249

Mane, S., Sapat, R., Kor, P., Shelar, J., Kulkarni, R. D., & Mundkar, J. (2020). Microcontroller based automatic power factor correction system for power quality improvement. *2020 International Conference for Emerging Technology, INCET 2020*, *6*, 7–12. https://doi.org/10.1109/INCET49848.2020.9154008

MarketsandMarkets. (2023). *power electronics market size, share*. https://www.marketsandmarkets.com/Market-Reports/power-electronics-market-204729766.html?utm

Medina-Gaitán, D. F. A., Rozo-Rodriguez, I. D., & Montoya, O. D. (2023). Optimal Phase-Balancing in Three-Phase Distribution Networks Considering Shunt Reactive Power Compensation with Fixed-Step Capacitor Banks. *Sustainability (Switzerland)*, *15*(1). https://doi.org/10.3390/su15010366

S Mani Kuchibhatla, V. V. S. L. S. V. A. N. (2022). IRJET- Compensation of Reactive Power and Energy Saving using Capacitor Banks. *Irjet*, *9*(1), 630–633.

Srikakolapu, J., Arya, S. R., Maurya, R., & Sharma, S. (2022). Predictive Control-Based DSTATCOM with a Multi-Criterion Decision-Making Method. *Journal of The Institution of Engineers (India)*, *Volume 103*, 2097–2110. https://doi.org/https://doi.org/10.1007/s40031-022-00800-z

Tang, Z., Yang, Y., Member, S., & Blaabjerg, F. (2022). *Power Electronics : The Enabling Technology for*. *8*(1), 39–52. https://doi.org/10.17775/CSEEJPES.2021.02850

X. Zhou, K. Wei, Y. M. and Z. G. (2018). Review of Reactive Power Compensation Devices. *018 IEEE International Conference on Mechatronics and Automation (ICMA), Changchun, China*, 2020-2024,. https://doi.org/10.1109/ICMA.2018.8484519

Y. Xu, X. Pan, J. Guo, X. S. and H. Z. (2023). Dynamic Reactive Power Characteristics Analysis and Optimization of Synchronous Condensers. *2023 10th International Forum on Electrical Engineering and Automation (IFEEA), Nanjing, China*, 484–488. https://doi.org/https://doi.org/10.1109/IFEEA60725.2023.10429104

Ye, L and Longfu, L. (2024). The Proceedings of the 18th Annual Conference of China Electrotechnical Society. In C. Tianjin University of Technology, Tianjin, Tianjin, Q. Yang, C. East China Jiaotong University, Nanchang, Jiangxi, Z. Li, C. Hunan University, Changsha, Hunan, & A. Luo (Eds.), *Research on Reactive Power Control of Synchronous Condenser Based on Sliding Mode Control* (pp. 614–623). Springer, Singapore. https://doi.org/https://doi.org/10.1007/978-981-97-1428-5_67

Zican Tao, T. W. and R. C. (2024). *Research on Reactive Power Optimization of Synchronous Conversion Factor*.